Mechanical behaviour of spun-cast grey iron pipe
Makar, J. M.; McDonald, S. E.

National Research Council Canada   Conseil national de recherches Canada

Canada

Mechanical behavior of spun-cast gray iron pipe

NRCC-50053

Makar, J.M.; McDonald, S.E.

National Research Council Canada   Conseil national de recherches Canada

The Mechanical Behaviour of Spun-cast Grey Iron Pipe

J.M. Makar* and S.E. McDonald[+]
Institute for Research in Construction
National Research Council Canada
1200 Montreal Road, Ottawa, Ontario K1A 0R6
Canada

Abstract

Past work has made little differentiation between the mechanical properties of pit and spun cast grey iron water pipes. Mechanical tests on coupons from spun and pit cast samples presented here show that spun cast grey iron has mechanical properties that fall between those of pit cast grey iron and ductile iron pipes, often with marked similarities to ductile iron. The properties determined from the mechanical tests were used to examine whether linear elastic analysis can be successfully used to approximate the mechanical behaviour of a pipe loaded in bending. Linear elastic analysis was found to produce reasonable approximations to the behaviour of undamaged pipes. The effect of corrosion pitting was included in the analysis by determining stress concentration factors for pits of varying depths at different stress levels. Multiplying the stress concentration factors by the results of the linear elastic analysis produced results with an error of no more than 6% from the values produced by a full cast iron plasticity analysis within the experimentally measured range of ultimate stresses.

*Corresponding Author
e-mail: jon.makar@nrc-cnrc.gc.ca

[+]Now at
City of Ottawa,
Drinking Water Services,
951 Clyde Ave.
Ottawa, Ontario
K1Z 5A6
Canada

1 Introduction

Grey cast iron is a legacy material in water mains throughout the world. Installed in Europe as early as the 1600s (Cast Iron Pipe Research Association, 1952), it was the dominant water main material from the mid 1800s to the 1950s and the water systems of most older urban centers continue to have a majority of their pipes made from grey cast iron. Failures are generally attributed to a gradual reduction over time in localized wall thickness through corrosion pitting (Makar, Desnoyers and McDonald, 2001). Other factors such as water pressure and temperature changes are also known to play a role in pipe failure.

Two primary types of casting methods (pit and spin casting) were used to produce grey cast iron pipes (Cast Iron Pipe Research Association, 1952). Pit casting typically involved the use of upright sand moulds assembled in pits. Spin casting used horizontal, spinning moulds, which were made of sand or metal. The metal moulds were water cooled, and promoted more rapid cooling of the pipes. The different casting methods produced profound differences in the metallurgy of the pipe material (Makar and Rajani, 2001). Pit cast iron typically has large ASTM type C flakes (ASTM, 1998), while spun cast pipes typically have much finer ASTM type D flakes throughout the bulk of the pipe wall, with a small amount of type C or A flakes on the inside surface of the pipe.

The mechanical properties of grey cast iron pipe were investigated in the 1920s and 1930s both as part of the development of the 1939 American Water Works Association (AWWA) standards on pipe design and as independent research. Perhaps the most important work was that of Talbot (1926), who studied pipes made by four different casting methods – vertical pit casting, horizontal casting, centrifugal casting in sand moulds and centrifugal casting in water cooled metal moulds. He examined the resistance of the sample pipes to internal pressure, in flexure and under impact conditions. He also presented the results from test specimens for bending, tensile, flexural and ring tests.

More recently, mechanical testing has been done on pipes removed from service in order to develop an improved understanding of the mechanical behavior of intact and partially corroded pipe. This work has largely been conducted in the context of making decisions about pipe replacement and rehabilitation. Research results have been presented by Kirkby (1977), Yamamoto (1983), the Philadelphia Water Department (1985), Jakobs (1985), Attewell (1986), Conlin and Baker (1991), Rajani et al., (2000), and by Seica and Packer (2004 a,b). Only the reports by Rajani et al. (2000) and Attewell (1986) clearly differentiated between measurements taken on the two types of pipes, while Kirkby (1977) reported solely on pit cast pipes. In general, the ultimate strengths of the tested samples were reported, not their stress-strain curves. Seica and Packer (2004a) show one stress-strain curve in tension and one in compression from their samples, but do not identify which type of cast iron was used to produce their results.

While the applicable standards require considerably greater strength in spun cast iron pipes (125/145 MPa) (AWWA, 1953) than pit cast (75 MPa) (AWWA, 1939), the way in which that greater strength is created does not appear to have been fully appreciated. In particular, the mechanical behaviour of spun cast grey iron does not follow that typically reported for grey cast irons (Iron Castings Society, 1981). Instead, it has mechanical behaviour that is generally closer

to that of ductile iron than that of pit cast iron pipes. Here, the tensile and compressive behaviour of typical and anomalous spun cast grey iron samples are discussed in detail, including both ultimate strengths and stress-strain curves.

The results of the experimental measurements were then used to explore whether linear elastic analysis can be used to approximate the mechanical behaviour of grey cast iron pipes under applied loads. Most failures in grey cast iron pipes can be attributed to loads that produce bending. Rajani and Tesfamariam (2004) and Tesfmariam and Rajani (2004) have used linear elastic analysis in order to analyze the bending behaviour of pipes in the ground while bypassing the computational expense of finite element analysis (FEA). However, results from Seica and Packer (2004b) suggest that linear elastic analysis can not be used to successfully model cast iron pipe behaviour. Here we describe an approach to the analysis of the bending behaviour of cast iron pipes that allows linear elastic analysis to be employed while still accounting for the plastic mechanical properties of the pipes.

2 Experimental Details

Multiple tensile coupons were cut from five spun cast grey iron pipes exhumed from the National Research Council Canada's Montreal Road, Ottawa campus during the course of a pipe replacement project. The pipes were all of 150 mm inside diameter and had been installed in the 1950s (more accurate dates were not available). Tensile coupons were also cut from a 100 mm inner diameter pit cast pipe from the city of Vancouver and from a commercially supplied ductile iron pipe. All samples were made to the dimensions in ASTM E8-94a (1994). While the standard allows for an alternative procedure for pipe coupons that maintains the curvature of the pipe wall and uses correspondingly curved grips, past work has shown that this procedure presents a high likelihood of inducing bending stresses during loading. Instead, the pipe walls

were flattened to allow the use of flat grips. Some samples had the minimum flattening possible, while others were deliberately thinned to 5, 7 or 9 mm in thickness to explore the effect of loss of wall thickness on the coupons' mechanical behaviour. As the natural pitting in these pipes was primarily on the interior of the pipe wall, the thinned samples were produced by removing the inner wall material once the outer wall had been flattened. Table 1 shows the number of samples used with each thickness. A large number of samples were taken from most pipes in order to investigate the degree of variation in the stress-strain curves. Grey cast iron is known to vary significantly in response between coupons taken from the same casting (Iron Castings Society, 1981).

The coupons were loaded in tension until failure following ASTM E8-94a, with data being collected using a computer based data acquisition system. Strain data was typically collected using an extensometer system during the tensile tests, but individual coupons without corrosion pits were also instrumented with strain gauges on both sides of the sample to ensure that no bending was taking place.

It is worth noting that since grey cast iron has lower ultimate strengths in tension than in compression, the tensile tests provide the best simulation of the failure conditions experienced by small diameter pipes in bending. The level of axial stress in a small diameter pipe at the point of maximum tension on the pipe varies by less than 6 % of the maximum value through the pipe wall and by less than 1% within first 40 mm along the pipe axis. In contrast, measurements made on four point bending coupons (also known in the water industry as Talbot strips) take place on a sample that goes from maximum compression to maximum tension across the pipe wall. The maximum tension experienced by the four point bending coupons is confined to one surface of the sample, making this test a less accurate representation of the local mechanical behaviour of an in-service pipe.

Cylindrical compression testing coupons were also cut from the spun and pit cast grey iron pipes. In general ASTM E8-89a (ASTM 2000) was followed for the compression tests. However, the thickness of the pipe wall did not allow for the cutting of standard test coupons. The minimum short sample size in the standard is a cylinder with a 0.5 in. (13 mm in the standard) diameter and a 1.0 in. (25 mm in the standard) length. Since the samples were taken from cast iron pipes with thickness ranging from 9 mm to 12.5 mm, a 13 mm diameter sample was impossible to obtain. Instead, samples were taken with the maximum possible diameter from each pipe with the length being maintained at twice the value of the diameter. Compressive measurements were made using the same testing machine, equipped with compressive testing platens rather than grips. Strain data was collected using strain gauges during the compression measurements.

Coupons were also taken from each grey cast iron pipe for metallographic analysis. Each metallography coupon was mounted in epoxy resin and polished according to standard procedures for grey cast iron (ASM, 1985). The microstructure of each sample was recorded for future reference. The graphite flake type and size were also determined according to the relevant ASTM standard (ASTM, 1998).

3   Experimental Results and Discussion

3.1   Metallography

Table 2 shows the ASTM flake types and sizes for each of the grey cast iron samples used for the work presented here. The pit cast pipe showed type C flakes, while the first three spun cast pipes had type D flakes with a small amount of fine type A or C flakes on the inner surface of the pipe. These structures are typical for these classes of pipe (Makar and Rajani, 2001). However, spun cast samples 4 and 5 showed an anomalous flake pattern, with the transition from

type D to type C flakes occurring about half way through the pipe (Figure 1). The type C flakes were also larger in these pipes than in the other spun cast samples.

The metallographic work also included imaging the interfaces between the corrosion products and the intact metal in pipes. Figure 2 shows an example of the interface near the inner surface of the spun cast pipe 3, where the adjacent metal has type C graphite flakes. The dark masses are the corrosion products. The separation of regions of corrosion by apparently intact metal was seen at all the corrosion/metal interfaces that were studied during the course of the research.

3.2 Mechanical Testing

Figures 3 and 4 show typical stress-strain curves in tension and compression, respectively, for a pit cast grey iron pipe and four different spun cast grey iron pipes. Figure 3 also shows a typical stress-strain curve for a ductile iron pipe, as well as results for an additional spun cast sample. The thin walls of the ductile iron pipe used in the experiment prevented usable compression samples from being obtained. The stress-strain curves for the pit cast pipe are typical of those expected from grey cast irons with Type A or C graphite flakes (Iron Castings Society, 1981). In contrast, all of the coupons from the spun cast grey iron pipes showed a distinct "knee" on their stress-strain curves, similar to that of ductile iron. The tests on coupons from spun cast pipes 1 to 3 also showed initial stress-strain slopes closer to those of the ductile iron sample than the pit cast sample, while tests on coupons from the pipes 4 and 5, which had anomalous metallography, showed stress-strain curves with values between those of the pit cast results and the results from the more typical spun cast pipe. The ratios of the ultimate compressive strength to tensile strength of the samples also show that the typical spun cast pipes behave mechanically in a manner more similar to ductile iron than pit cast grey iron. Ductile iron

is typically about 20% stronger in compression than tension, while pit cast grey iron can be between 2 to 2.5x stronger (Iron Castings Society, 1981). A comparison of the data in Figures 3 and 4 show that spun cast grey iron pipes 1 to 3 are approximately 1.3-1.5x stronger in compression than tension, with pipe 4 being about 1.7x stronger.

In contrast, the ultimate strain behaviour of the spun cast pipes was closer to the pit cast pipe behaviour than that of the ductile iron. Tested ductile iron samples had ultimate strains between 1.5 and 4% in tension, which correspond well to standard values for this material. None of the spun cast grey iron pipe samples had ultimate strains of more than 0.9% in tension. The maximum ultimate strain measured for a pit cast sample in tension was about 0.4%, as shown in Figure 3.

The differences between the mechanical behaviour of spun cast pipes 1 to 3 and spun cast pipes 4 to 5 wre investigated by tested thinned samples. In coupons from the first three spun-cast pipes, the effect of thinning the coupon was to change the ultimate stress and strain of the sample without changing the shape of the stress-strain curve itself. Figure 5 shows a series of stress-strain curves measured on coupons taken from spun cast pipe 3, with similar results being obtained from pipes 1 and 2. All of the measured stress-strain curves for each pipe follow approximately the same slope, with the visible variation being expected for grey cast irons (Iron Castings Society, 1981). The thinnest samples had the highest ultimate stress and strains, with increasing thickness producing lower ultimate values. This variation is also expected, since coupons with a small cross section taken from the same source are known to experience higher ultimate stresses than larger cross section coupons (Iron Castings Society, 1981).

Spun cast pipes 4 and 5 show a different type of behaviour with increasing thickness. In the case of spun-cast pipe 4 (Figure 6), the 5 mm and 7 mm thick coupons have comparable ultimate strains, even though they do not have the same ultimate stresses. A single example of both the 9

mm thick and surface thinned samples also have the same ultimate strain, but again with lower ultimate stresses than the thinner samples. The other 9 mm and surface thinned coupons have reduced ultimate strains, but the clear pattern of behaviour seen in Figure 5 is not apparent. The results from spun-cast pipe 5 are similar.

The use of thinned samples in this work was intended only to explore the effect of the flake type distribution in the samples on their mechanical properties. The thinned samples should not be taken as being representative of the measurements to be expected from pitted samples. In the latter case, stress concentrations due to the presence of the pits and to the rough interface zone (Figure 2) between the corrosion product and the uncorroded metal will change the macroscopic stress-strain curves measured during a tensile test.

3.3   Discussion of experimental results

The mechanical behaviour of grey cast iron has generally been attributed to the complex interaction between the graphite flakes and the metallic matrix. Although there is some divergence of opinion on the details, there is general consensus that the graphite flakes act as sources of stress concentration in the metal, inducing plastic deformation at much lower stresses than would be the case in a steel with similar alloy content. One of the most commonly accepted models (Angus, 1976) of micromechanical behaviour suggests that the macroscopic mechanical behaviour of the material is produced by strains in both the metal and in the voids that form at the surfaces of the flakes as the object under investigation is loaded (i.e. there are reversible and irreversible openings of voids at the graphite flake interfaces as well as reversible and irreversible strains in the metal matrix).

Examining Figures 3 and 4 clearly shows that the spun cast grey iron pipes have mechanical behaviour that falls part way between that of ductile iron pipes and pit cast grey iron pipes. In

tension (Figure 3), the pipes that had type D graphite flakes throughout almost all of the pipe wall (spun cast pipes 1 to 3) had the closest behaviour to ductile iron, with similar, although slightly lower, ultimate strengths and noticeable knees in their stress-strain curves. The pipes with approximately 30% of the pipe wall composed of type C flakes (spun cast pipes 4 and 5) still had noticeable knees in their stress-strain curves, but their ultimate strengths and strains were lower and closer to those of the pit cast pipe. In compression (Figure 4) all four spun cast pipes tested had similar behaviour, with noticeable knees and ultimate strengths less than that of the pit cast pipe. The ratio of the compressive to tensile ultimate strengths of the spun cast pipe material was also found to fall between the values expected for ductile iron and pit cast grey iron.

These results suggest that stress concentrations at the smaller, Type D graphite flakes in the spun cast grey iron pipes produce less initial plastic deformation than the larger type C flakes in the pit cast iron pipe. The stress concentration effect of the graphite in ductile iron is minimized by its spherical shape. While the type D flakes still act as stress concentration sites, their impact is reduced by both their smaller size and their clustered distribution. The results of Figures 5 and 6 show the significance of the type C flakes. In Figure 5, the measured stress-strain curves fall within a tight envelope of values and reducing the thickness of the coupons simply increases the ultimate stress and strain of the material. The thicker samples with additional graphite flakes and a change of flake type at the outer surface provide more opportunities for failure to initiate, but do not significantly affect the underlying mechanical behaviour of the pipe. In Figure 6, thinning the coupons produces a change in the stress-strain curve itself. The surface flattened coupons and the 9 mm thick coupons show the full effect of the type C flakes. The 7 mm thick coupons have most of the metal with type C flakes removed, while the graphite in the 5 mm thick coupons is composed solely of type D flakes. Removing the type C flakes both increases the ultimate stress of the material and increases the slope of its initial stress-strain curve.

A simplistic analysis would suggest that this effect was due to the removal of the weaker material and that the observed stress-strain curve in the full thickness samples could be determined from the stress-strain curve of the material with the type D flakes in combination with the stress-strain curve of the material with type C flakes. However, the differences between the samples with and without the type C flakes are so large that such an explanation would require that the region of cast iron with type C flakes had essentially no strength at all. This is unlikely to be the case, as the regions of type C flakes in these samples exhibited typical metallography, with a matrix of continuous metal and smaller graphite flakes than are found in the pit cast sample. Instead, these results suggest that the larger graphite flakes in the type C region affected the plastic deformation behaviour of the entire sample. Plastic deformation was more likely to initiate near the larger, type C flakes, but once it had initiated, it then occurred throughout the sample.

4 Finite Element Analysis

The experimental stress-strain data presented here allows for a more comprehensive investigation than has previously been possible of the question of whether linear elastic analysis can be used to approximate the response of grey cast iron pipes to mechanical loading and determine their risk of failure. Small diameter grey cast iron pipe failures are almost always associated with corrosion pitting or casting flaws (Makar, Desnoyers and McDonald, 2001). These pits produce significant local stress concentrations, but do not affect the overall response of the pipe to external loads. A possible approach to determining the vulnerability of a pipe to failure would therefore be to analyze the response of an undamaged pipe to external loads and then multiply the maximum obtained stress from that calculation by a stress concentration factor (SCF), which would represent the additional stress concentration effects due to the presence of damage in the pipe. This approach would not give any particular advantage in an analysis of a

linear elastic material. However, in cases such as grey cast iron pipes, where plastic deformation plays a significant role in the response to applied stress, a significant computational advantage could be produced by allowing much of the computation to be done using linear elastic analysis. If appropriate SCF values can be determined that take into account the effects of grey cast iron plasticity, a linear elastic analysis would need only to closely approximate the behaviour of the undamaged pipe in order to be useful.

As a test of the proposed approach, finite element analysis of a 3 m. long, 150 mm inner diameter pipe loaded in bending (Figure 7) was undertaken using the Abaqus® software package, which contains a full grey cast iron plasticity model based on the work of Hjelm (1994) and validated against experimental data both by the developers and in independent research (Makar, et al., 2005). The latter work was done using a finite element analysis (FEA) of the mechanical behaviour of a corrosion pitted, 3 meter long, 150 mm diameter pipe placed in bending similar to that considered here. In contrast, the FEA reported here investigated undamaged pipes and pipes with a single 20 mm diameter pit located at the point of maximum bending in tension using both full plastic analysis and an approximation based on linear elastic analysis. The measured stress-strain curves in Figures 3 and 4 for the pit cast pipe and spun cast pipe 3 were used for the analysis.

The first step in testing the proposed approach was to determine the applicable SCFs, which varied based on both the dimensions of the corrosion pit and the stress in the undamaged pipe. Figures 8 and 9 show the SCFs taken from the finite element analysis for pit and spun cast pipes respectively as functions of the stress in the undamaged pipe. The plastic behaviour of the grey cast iron under applied stress caused the SCF values to fall with increasing stress. The rate of change in the factor was found to be dependent on the slope of the stress-strain curve at both the

underlying stress in the pipe and the maximum value experienced near the pit. A large difference between the two produced a steeper slope in the graph.

The second step was to determine whether linear elastic analysis can approximate the behaviour of an undamaged pipe, which, for the same applied loads, would experience much lower maximum stresses than a pipe with corrosion pitting. As shown in Figure 10, it was possible to choose an appropriate elastic modulus value for use in an linear finite element analysis that produced approximately correct mechanical response to loading for a wide range of deflections and corresponding stresses within both pit and spun cast pipes.   The two elastic curves shown in Figure 10 are examples, since the precise curve chosen for an analysis of a pipe in the ground would depend on the range of stresses or deflections expected to be experienced by that pipes.

Finally, Figure 11 shows a direct comparison of the results of multiplying the stress concentration factors by the linear curves in Figure 10 to the results produced by a full cast iron plasticity analysis. The location of the measured ultimate strengths from the tensile tests for each pipe material are also shown for the purposes of comparison. The linear elastic analysis/stress concentration factor approach gave a close approximation to the results of the full analysis, with an error of no more than 6.5%.

In summary, the analysis here showed that it was possible to model grey cast iron pipe behaviour using a linear elastic approximation. In addition to typical stress-strain curves, two outside pieces of information would be necessary if the goal of such an analysis is to quickly model pipe behaviour in an operating water network. First, information on typical pit dimensions associated with pipe failures in the network must be obtained. These dimensions can be used to determine stress concentration factors similar to those in Figures 8 and 9 that are representative of failure conditions. Secondly, an acceptable level of stress within the pipe needs to be determined.

This could be based on the minimum ultimate stress measured during the development of the stress strain curves (here 125 MPa and 167 MPa for the pit and spun cast pipes respectively), set to produce an appropriate factor of safety below the minimum ultimate stresses or determined by other means. Examples of undamaged pipes could then be analyzed under the various loading conditions experienced within the water network and pipes at risk of failure found by comparing the stress in the undamaged pipe multiplied by the appropriate stress concentration factor to the selected failure criteria.

5 Conclusions

Although most researchers have treated treated pit and spun cast pipes as having identical mechanical properties, there are significant differences between the two types of pipe material. In particular, typical spun cast iron samples have:

- A steeper initial stress-strain curve in both compression and tension than pit cast iron;
- a "knee" in its stress-strain curves;
- a higher ultimate strength and ultimate strain in tension than pit cast iron; and
- a lower ultimate strength but higher ultimate strain in compression than pit cast iron.

In all these points, the mechanical behaviour of spun cast iron was found to fall between that of pit cast iron and ductile iron. The differences in mechanical behaviour were attributed to differences in the graphite flake types between the different classes of pipes. Only anomalous spun cast irons, with atypical cast iron flake types and distributions, had mechanical behaviour that was closer to pit cast iron than ductile iron.

While linear elastic analysis alone is clearly inappropriate as a method of modeling the mechanical behaviour of damaged grey cast iron pipes, using such an analysis in combination with stress concentration factors that represent the effects of the damage can approximate responses to external loads with minimal error. As this approach would require substantially

fewer computation resources than a full grey cast iron plasticity analysis, extensive modeling of operating pipe networks to determine vulnerabilities to failure would become possible. Stress concentration factors would need to be determined based on the size of corrosion pits typically associated with a pipe failure. The calculated stresses in pipes under different loading conditions could then be compared to an acceptable level of stress in the pipe to determine if rehabilitation work is warranted.

Acknowledgements

References

Angus, H.T., 1976. *Cast Iron: Physical and Engineering Properties*. 2nd Edition, Butterworths, London, pp. 54-79.

ASTM (American Society for Testing and Materials), 1994. *Standard testing methods for tension testing of metallic materials*. ASTM E8-94a. New York: American Society for Testing Materials.

ASTM (American Society for Testing and Materials), 2000. *Standard test methods compression testing of metallic materials at room temperature*. ASTM E9-89a. New York: American Society for Testing Materials.

ASTM (American Society for Testing and Materials), 1998. *Test method for evaluating the microstructure of graphite in iron castings*, ASTM 247-67, New York: American Society for Testing Materials.

AWWA, 1939. (American Water Works Association). *American Standard Practice for the Computation of Strength and Thickness of Cast-Iron Pipe*. ANSI/AWWA A21.1-39. Denver, CO: American Water Works Association.

AWWA, 1953. (American Water Works Association). *American Standard Practice for the Computation of Strength and Thickness of Cast-Iron Pipe*. ANSI/AWWA A21.1-53. Denver, CO: American Water Works Association.

Cast Iron Pipe Research Association, 1952. *Handbook of Cast Iron Pipe for Water, Gas, Sewage and Industrial Services*. Chicago, Illinois.

Conlin, R.M. & Baker, T.J., 1991, *Application of fracture mechanics to the failure behavior of buried cast iron mains*. Contract Report 266. London: Transport and Road Research Laboratory.

Iron Castings Society, 1981. *Iron Castings Handbook,* Chapter 6, Iron Castings Society.

Hjelm, H.E., 1994. Yield surface for grey cast iron under biaxial stress, *Transactions of the ASME: Journal of Engineering Materials and Technology*, 116(2): 148-154.

Jakobs, J.A., 1985. Underground Corrosion of Water Pipes in Canadian Cities – Case: The City of Calgary, Final Report, Caproco Corrosion Prevention Ltd., (CANMET Contract Report No. 0SQ81-00096, Canadian Centre for Mineral and Energy Technology, Energy, Mines and Resources Canada). Ottawa, Canada: Canadian Government Publishing Centre.

Kirkby, P.C., 1977. *Internal Corrosion and Loss of Strength of Iron Pipes*. Paper 10. Swindon, England: Water Research Centre.

Makar, J.M., Desnoyers, R., and McDonald, S.E., 2001. Failure modes and mechanisms in grey cast iron pipe, in *Underground Infrastructure Research: Municipal, Industrial and Environmental Applications.* Edited by M. Knight and N. Thomson, Lisse, The Netherlands: A.A. Balkema.

Makar, J.M. et al., 2005. *The Effect of Corrosion Pitting on Circumferential Failures in Grey Cast Iron Pipes*, Awwa Research Foundation, Denver, CO.

Makar, J. & Rajani, B., 2001. Grey Cast Iron Pipe Metallurgy, *Journal of Materials in Civil Engineering*, 12(3): 245-253.

Philadelphia Water Department, 1985. *Water Main Pipe Sample Physical Testing Program.* Denver, CO: AwwaRF and AWWA.

Rajani, B. et al., 2000. *Investigation of Grey Cast Iron Water Mains to Develop a Methodology for Estimating Service Life.* Denver, CO: AwwaRF and AWWA.

Rajani, B., and Tesfamariam, S., 2004. *Uncoupled axial, flexural, and circumferential pipe-soil interaction analyses of jointed water mains*. Canadian Geotechnical Journal, 41, 997-1010.

Seica, M.V. and Packer, J.A., 2004a. *Mechanical Properties and Strength of Aged Cast Iron Water Pipes*, Journal of Materials in Civil Engineering, 16(1): 69-77

Seica, M.V. and Packer, J.A., 2004b, *Finite Element Evaluation of the Remaining Mechanical Strength of Deteriorated Cast Iron Pipes*, Journal of Engineering Materials and Technology, 126 (1): 95-102.

Talbot, A.N., 1926. *Strength Properties of Cast Iron Pipe Made by Different Processes as Found by Tests*. Jour. AWWA, 16: 1-44.

Tesfamariam, S., and Rajani, B., 2004. *Impact of Uncertainties on the Translation of Remaining Pipe Wall Thickness to Structural Capacity* INFRA 2004 Urban Infrastructure: Managing the Assets, Mastering the Technology (Montreal, Quebec, 11/15/2004).

Yamamoto, K., Mizoguti, S. & Yoshimitsu, K., 1983. Relation Between Graphitic Corrosion and Strength Degradation of Cast Iron Pipe. *Corrosion Engineering,* 32(3): 157.

Tables

Sample	Total Number of Coupons	Coupon Thickness (mm)	Number of Coupon at Thickness
Pit Cast	5	6	1
		7	1
		8	3
Spun Cast 1	20	5	16
		Full (12.7)	4
Spun Cast 2	25	5	12
		7	6
		Full (9)	7
Spun Cast 3	5	Full (8)	5
Spun Cast 4	25	5	12
		7	5
		9	4
		Full (9.7)	5
Spun Cast 5	33	5	8
		7	12
		9	8
		Full	5

Table 1: Tensile testing coupon numbers and thicknesses

Sample	ASTM Flake Type[1]			ASTM Flake Size[2]		
	Inner Surface	Center	Outer Surface	Inner Surface	Center	Outer Surface
Pit Cast	C	C	C	4	4	4
Spun Cast 1	A	D	D	6	8	7
Spun Cast 2	C	D	D	5	7	8
Spun Cast 3	C	D	D	5	8	8
Spun Cast 4	C	C to D	D	4	5 to 8	8
Spun Cast 5	C	C to D	D	4	5 to 8	8

[1]In ASTM A247 the flake type indicates how the graphite flakes are distributed in the metal matrix. Type A indicates uniformly distributed, apparently randomly oriented flakes; type C indicates randomly oriented flakes of widely varying sizes and type D a very fine pattern of flakes surrounding areas without graphite.

[2]In ASTM A247 the sizes refer to a range of values as measured at 100x magnification that vary geometrically from 1 mm to 128 mm. Size 3 corresponds to approximately 16-32 mm at this magnification, size 4 to 8-16 mm, size 5 to 4-8 mm, size 6 to 2-4 mm, size 7 to 1-2 mm and size 8 to 0-1 mm.

Table 2: ASTM standard flake types and sizes

Figures
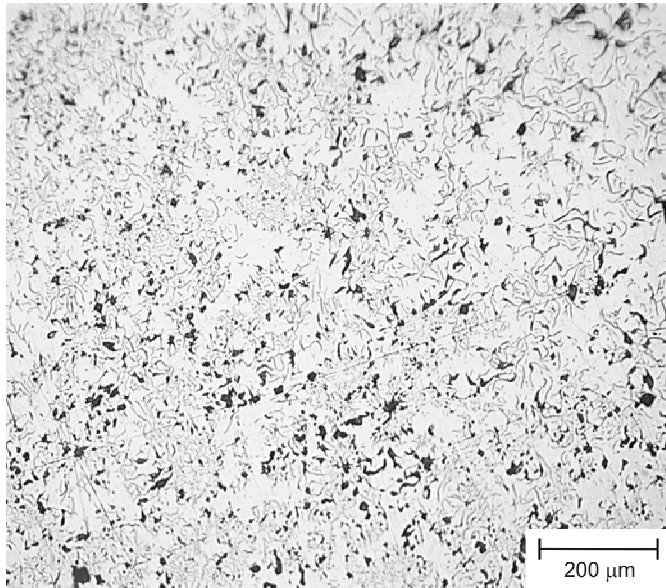
Figure 1: Transition between type C (upper right)and type D (center and lower left) flakes in spun cast pipe 4.
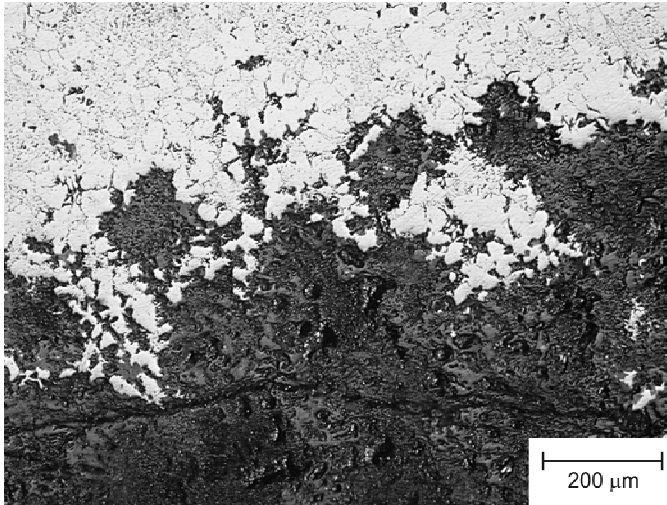
Figure 2: Interface between corrosion products (dark colour) and cast iron (light colour with dark flakes) in a spun cast pipe.
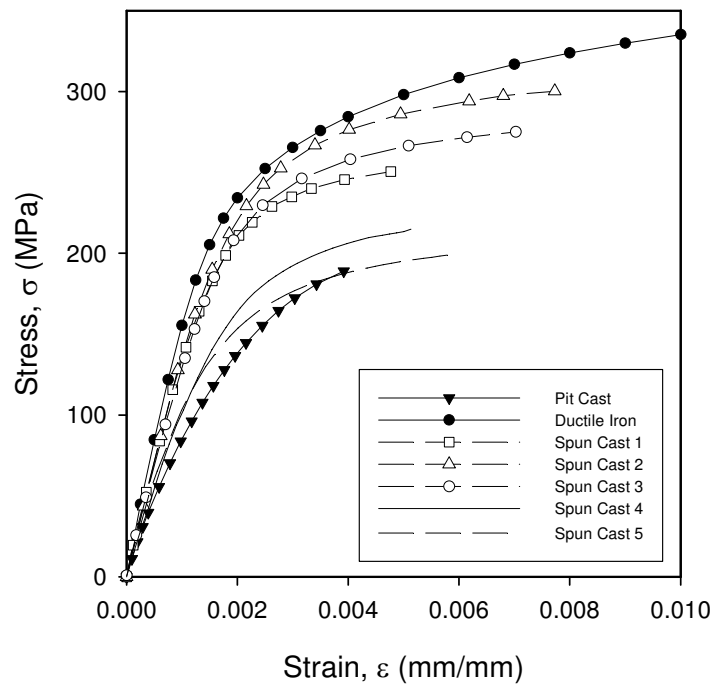
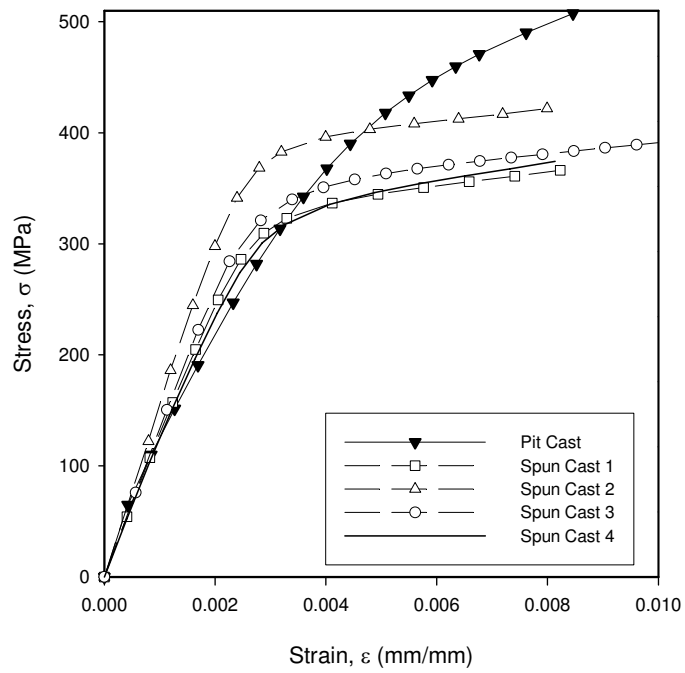Figure 3: Typical tensile stress-strain curves for pit cast pipe, spun cast samples and ductile iron

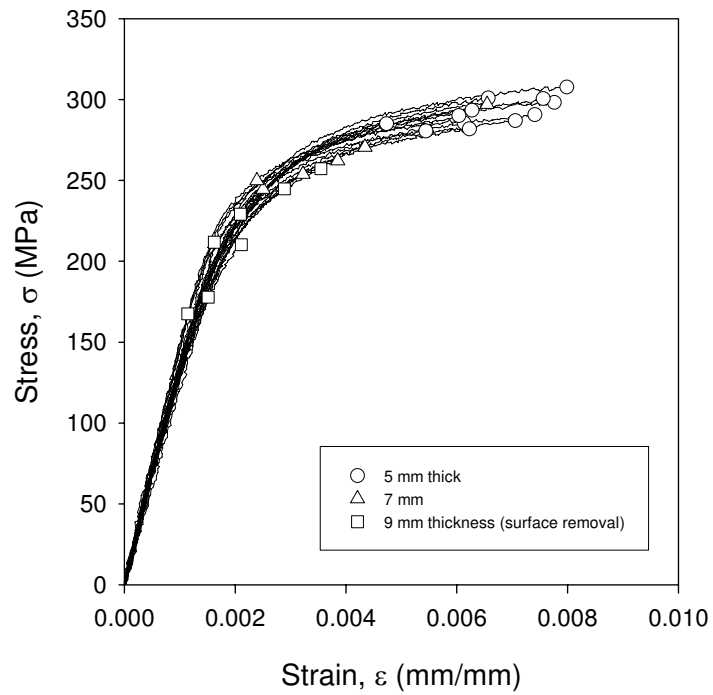Figure 4: Typical compressive stress-strain curves for pit and spun cast samples

Figure 5: Distribution of tensile stress-strain curves and failure points in typical spun cast iron
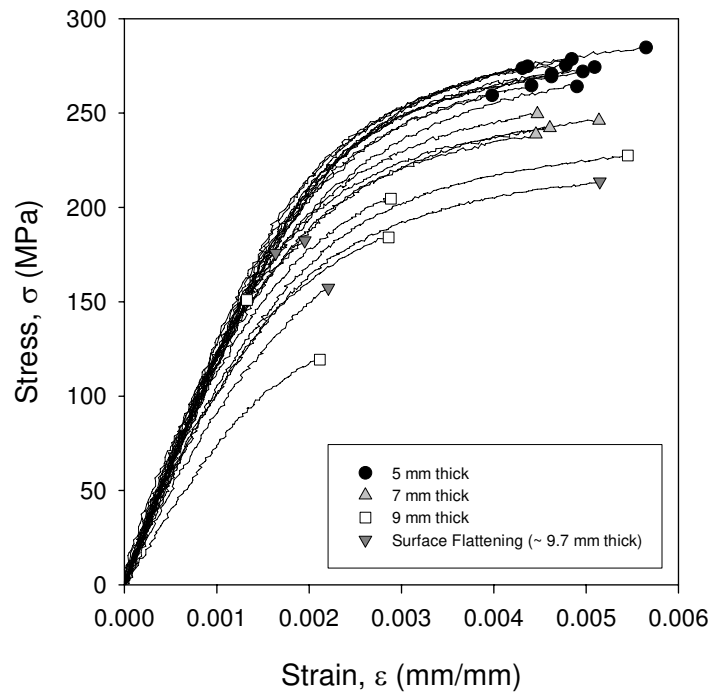
samples

Figure 6: Distribution of tensile curves in atypical spun cast samples, including effect of thinning
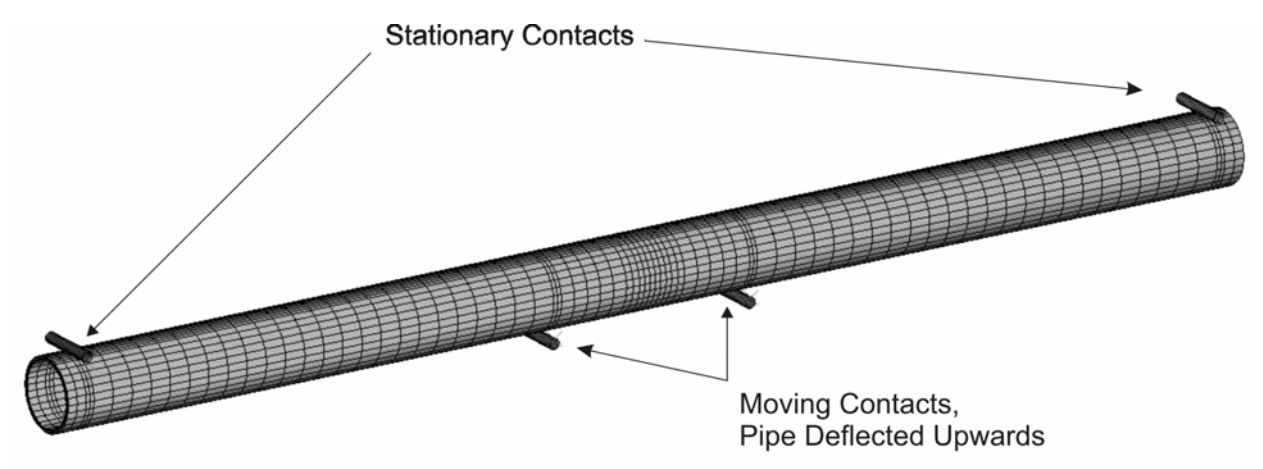
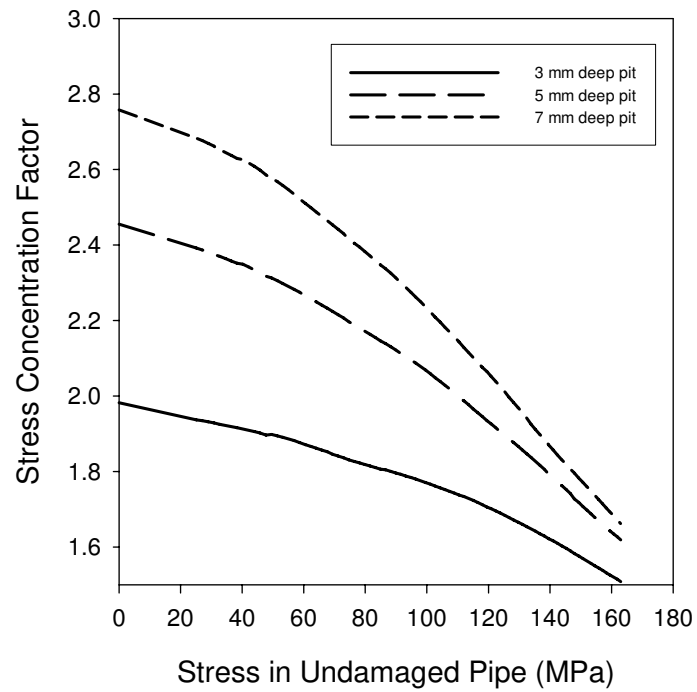Figure 7: Model of 3 meter long pipe loaded in bending used for finite element analysis

Figure 8: Effect of pit depth on stress concentration factors in 150 mm inner diameter pit cast
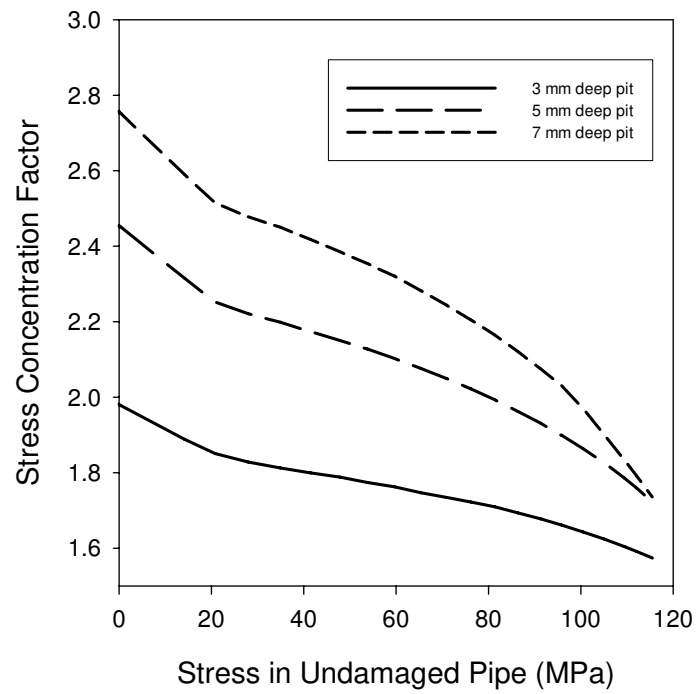
pipe with a 20 mm diameter pit

Figure 9: Effect of pit depth on stress concentration factors in 150 mm inner diameter spun cast

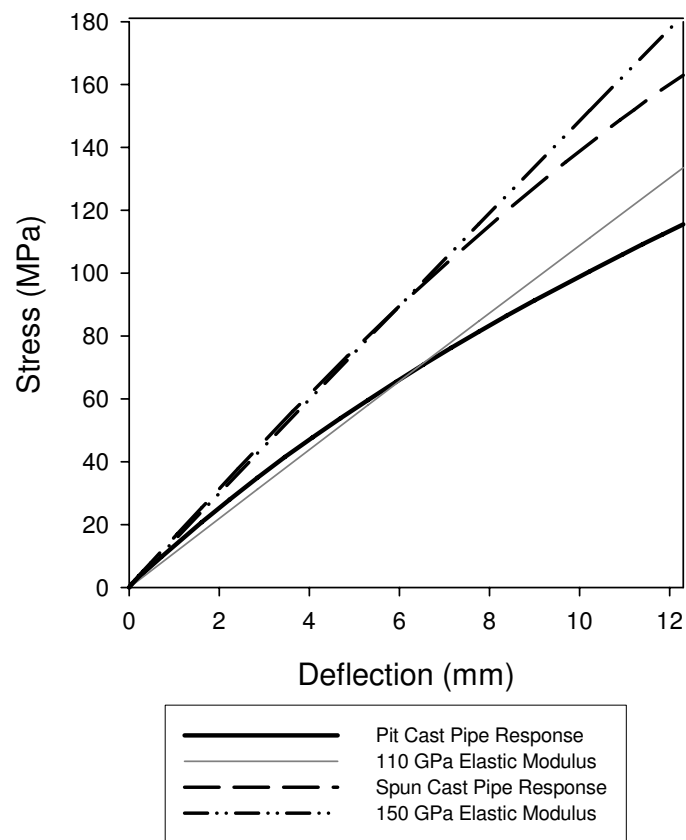pipe with a 20 mm diameter pit

Figure 10: Analysis of the response of a 3 meter long, 150 mm inner diameter pipe to a 12.3 mm
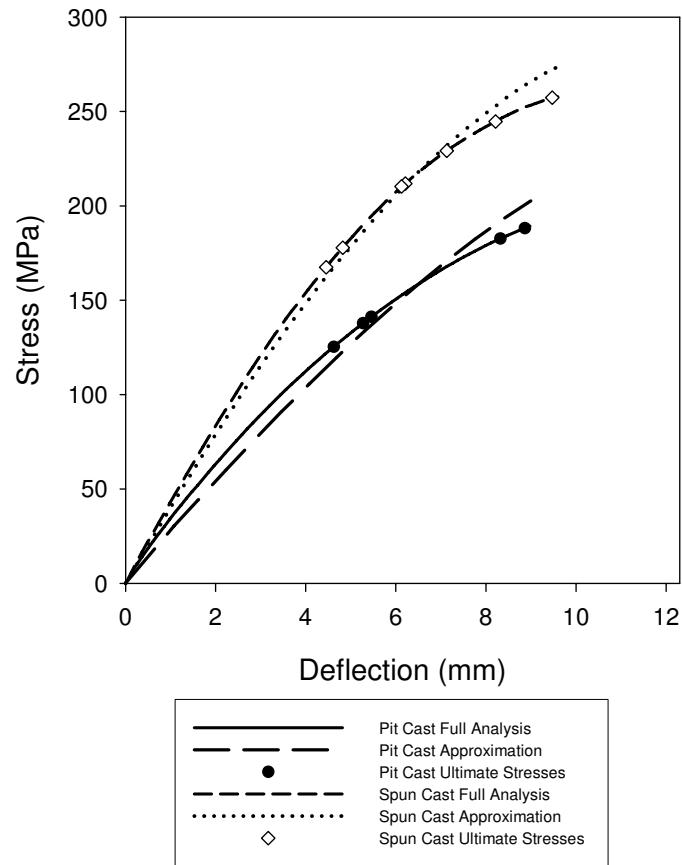
deflection

Figure 11: Comparison between results of proposed approximation and a full analysis using a
grey cast iron plasticity model. The analysis terminates when the largest measured
ultimate stress for each material is reached.